

OKAY
D.B.

C-Coupon Studies of SiC/SiC Composites Part II: Microstructural Characterization

Frances I. Hurwitz and Anthony M. Calomino
NASA Glenn Research Center
Cleveland OH, 44135

Terry R. McCue
QSS Group Inc.
Cleveland, OH 44135

Gregory N. Morscher
Ohio Aerospace Institute
NASA Glenn Research Center
Cleveland OH, 44135

ABSTRACT

A "C-coupon" was used to measure the interlaminar tensile behavior of five different composite materials: Sylramic/MI (melt infiltration SiC matrix), ZMI/MI, Sylramic/S300, and ZMI and Hi-Nicalon with an S200 matrix at room temperature, 816°C and 1204°C. Fracture behavior was characterized by field emission scanning electron microscopy, and observed cracking compared with events measured by modal acoustic emission. Both radial and matrix hoop cracking along the inner radius arising from hoop stresses were observed for all material types. In those composites in which the radial cracks were sufficiently wide to view the composite interior, fracture was observed to occur at the fiber BN or BN matrix interface.

INTRODUCTION

The "C-coupon" geometry[1-4] provides a specimen for measuring the interlaminar tensile behavior at elevated temperatures, and assessing the fabrication of composites around specific bend radii, where matrix infiltration may not be identical with that achieved in flat panels. Analysis of the stress distribution in this coupon[5] and initial microstructural analysis of a Sylramic/MI composite[6] have been presented previously. The present paper extends this work to a characterization of the fracture behavior of additional ceramic composites, and is accompanied by a companion study of modal acoustic emission which follows sequential cracking.[7] The focus of this paper is on characterization of specimens after ultimate failure using field emission scanning electron microscopy and energy dispersive spectroscopy.

EXPERIMENTAL

The "C-coupon" geometry, shown in Figure 1, was identical with that used in previous studies[5, 6]. Five different SiC/SiC composite systems were studied, which included two different SiC matrices and three different fiber-types. Melt-infiltrated (MI) SiC C-coupon composite specimens were fabricated by Honeywell Advanced Composites (Newark, DE) with Dow Corning Sylramic® and Ube Industries Tyranno ZMI fiber-types.

This is a preprint or reprint of a paper intended for presentation at a conference. Because changes may be made before formal publication, this is made available with the understanding that it will not be cited or reproduced without the permission of the author.

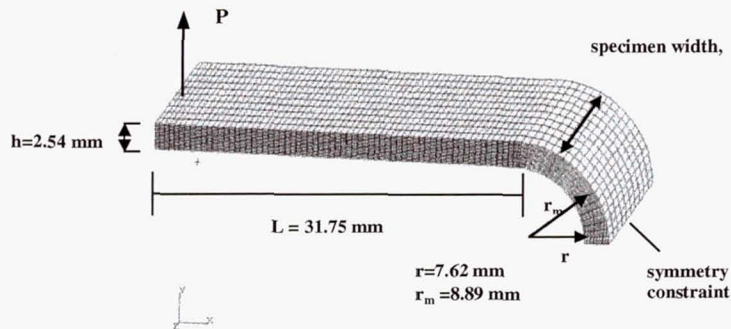


Figure 1. C-coupon geometry.

These composite systems will be referred to as SYL-MI and ZMI-MI, respectively. Polymer-infiltration pyrolysis (PIP) SiC C-coupon composite specimens were fabricated by COI Ceramics (San Diego, CA) with Sylramic fiber and the S300 SiNC matrix, and ZMI and Nippon Carbon Hi-NicalonTM fibers reinforcing an S200 (SiNC) matrix. All composites used eight plies of 5 HS weave cloth. All contained a BN interphase coating. The MI composites also contained a second CVI SiC coating over the BN.

Specimens were tested at 21, 816 and 1204°C. Testing was conducted at 21, 816 and 1204°C by Southern Research Institute, Birmingham, AL.. Modal acoustic emission (AE), as described in Part I,[7] was used to monitor cracking events. Hoop and radial stresses at failure were calculated based on finite element analysis of the C-coupon, as described previously.[5]

Fractured specimens were characterized by optical microscopy of polished section, field emission scanning electron microscopy (FESEM, Hitachi S4700 operated at 6kV) and by energy dispersive spectroscopy (EDS).

RESULTS AND DISCUSSION

Finite element analysis of the C-coupon[5] has shown that the radial stress is at maximum at the centerline of the C and at mid-thickness, while the hoop stress reaches a maximum at the centerline of the specimen on the inner radius (Fig 2). The C-coupon is expected to fail in interlaminar tension within the curved region of the coupon, provided that the ratio of the interlaminar to in-plane strength is less than 0.064, the ratio for the radial to hoop stress for a specimen configuration with a mean radius (8.89 mm) and thickness of 2.54 mm. This ratio can be estimated for a given composite from that of the ILT strength, determined from measurements on flat panels, to the in-plane tensile strength. A finite element analysis of the stress distribution in the more traditional "button specimen" (ASTM C1468), is provided by Carlsson.[1]

A comparison of maximum hoop and radial stresses, as calculated for the C-coupons based on the finite element analysis, and ILT data, determined using a "button test" is shown in Table I. Also included in this table is the ratio of ILT/ tensile strengths. In all composite systems for which room temperature tensile and ILT "button test" data was available, this ratio is substantially less than the 0.064 criteria needed for interlaminar fracture to be the dominant failure mode. In the case of ZMI/ S200, the 816°C tensile strength used in the ratio, as room temperature, it is likely that the C-coupon geometry thickness employed here also is valid for this composite system (a

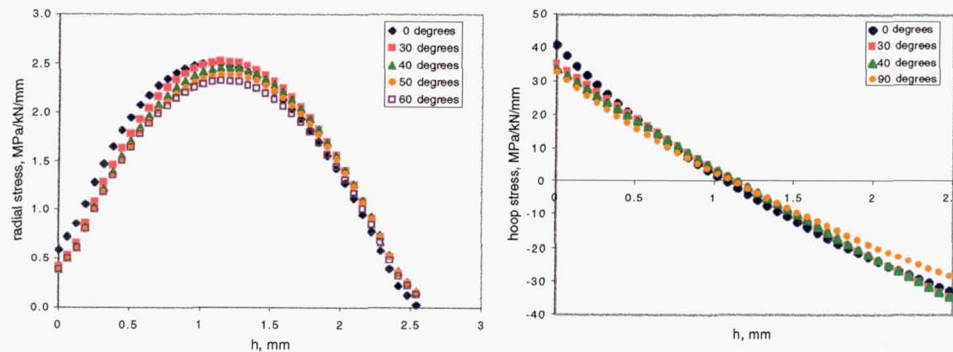


Figure 2. Stress distribution in C-coupon as a function of location within coupon.

room temperature tensile strength of 198 MPa would be required for the criterion to be met.). There is very good agreement between the maximum radial stress for the C-coupon specimens at room temperature, and the ILT "button test" result for all the composite systems.

Change in maximum radial stress as a function of temperature is plotted in Fig. 3. The MI composites showed a decrease in maximum radial stress at failure with test temperature. Sylramic/ MI decreased from 16 MPa at room temperature to 9 MPa at 1204°C; the ZMI appears as though there is a decrease in maximum stress with temperature as well, although there is more scatter. In contrast, the PIP composites did not exhibit a decrease in maximum radial stress with temperature. At all temperatures, ZMI/ MI composites were weaker than their Sylramic reinforced counterparts. In the PIP matrix systems, there was no significant difference in maximum radial stress between Sylramic and ZMI, but the Hi-Nicalon system was substantially weaker. As the "button test" cannot be used, there is no clear method for determining the ILT/tensile ratio at

Table I: Comparison of composite properties at room temperature.

Composite	Max Radial Stress, MPa	Max Hoop Stress, MPa	In- Plane Tensile Strength, MPa	ILT, MPa	ILT/Tensile
Sylramic/ MI	16.3 ± 1.0	269 ± 12	362 ± 25.5 ¹	15.5 ± 1.8	0.042
ZMI/ MI	12.5 ± 2.4 ²	203 ± 39 ²	N/A	N/A	N/A
Sylramic/ S300	15.9 ³	265 ³	317 ⁴	11.9 ± 0.6	0.037
ZMI/ S200	12.7	170	162 ± 9.4 ¹	12.7 ± 2.7	0.078
HiNicalon/ S200	8.5	120	248 ⁴	6.9 ⁴	0.027

¹ 816°C data.; room temperature strength expected to be equal or higher.

² Data is from one log only; the second log contained large pores.

³ Single data point—second sample failed at very low stress.

⁴ COI data.

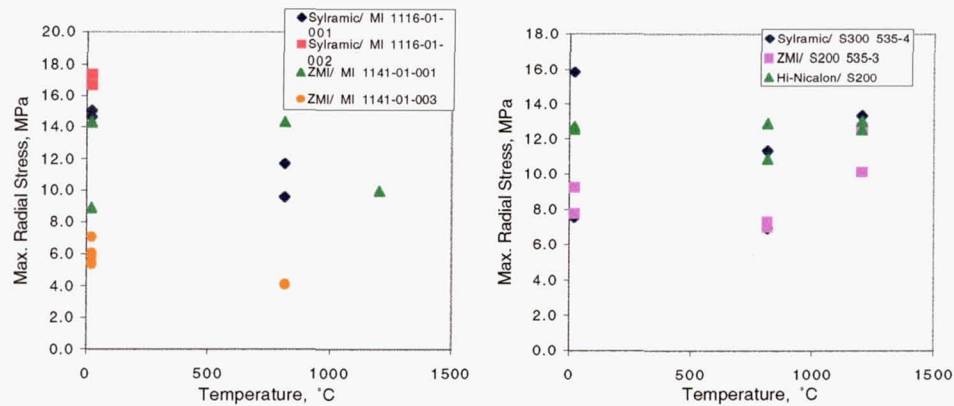


Figure 3. Maximum radial stress as a function of temperature. MI composites, right, and PIP composites, left.

elevated temperatures, or if the " < 0.064 " criterion is met, so determination of mode of fracture is based on microstructural evaluation. Analysis of the first fracture event for each composite material, as determined by AE, is presented in the companion paper.[7] For the Sylramic reinforced materials, there was no significant difference in first cracking stress between the MI and S300 matrices.

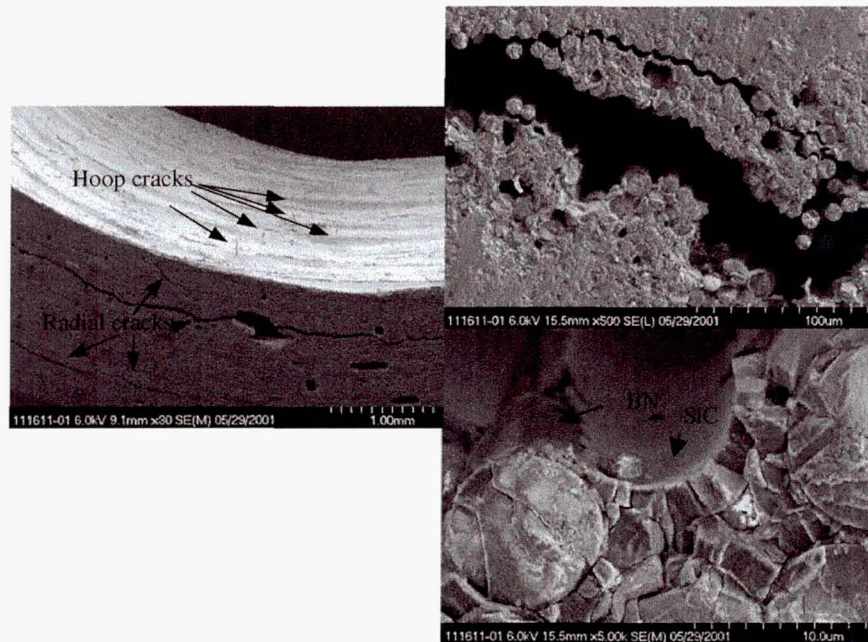


Figure 4. Fracture surface, Sylramic/MI tested at room temperature. Cracks due to radial stresses are on coupon edge; those arising from hoop stresses are located on inner radius.

Microstructural analysis was carried out using FESEM to determine the mode of failure. Room temperature fracture of the Sylramic/ MI composite is shown in Fig 4. A series of parallel radial cracks are observed, as well as a number of finer hoop cracks along the inner radius parallel to the width of the coupon and close to the center line. Because only coupons taken to failure were examined, it is not possible from the data available here to determine which set of cracks occurred first, or if they occur simultaneously. By looking down into several of the wider cracks, it can be seen that the "interlaminar" fracture occurs between the BN interphase and the CVI SiC overcoating, as confirmed by EDS. The CVI overcoat shows extensive cracking (Fig. 4, lower right), which might be the source of the very large number of AE events measured for the MI materials as compared with the polymer- derived matrix composites. At higher

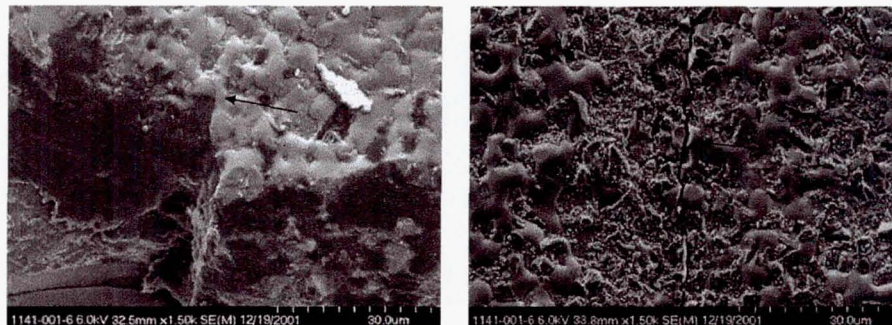


Figure 5. ZMI/ MI showing narrow hoop crack originating from matrix "notch".

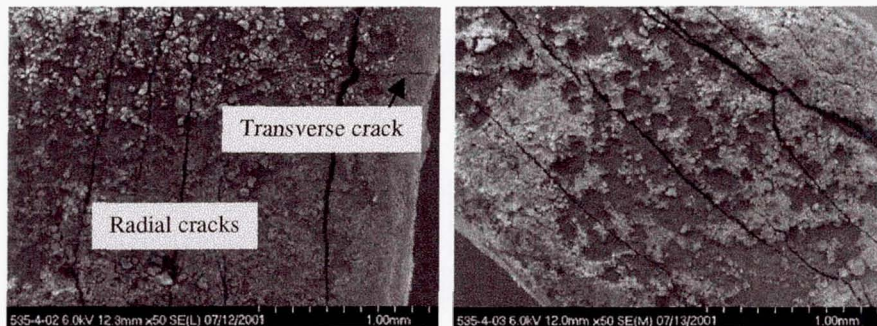


Figure 6. Sylramic/S300 fractured at room temperature (left) and 816°C (right).

temperatures, fewer radial cracks were observed, corresponding with a decrease in the maximum radial stress. Fracture behavior of the ZMI/ MI material is similar (Fig. 5), except that in this case the interphase fracture is between the fiber and the BN, and hoop cracks are extremely narrow ($0.05\mu\text{m}$). A Sylramic/ S300 composite tested at room temperature (Fig. 6, left) showed a higher density of radial cracking than the MI, as well as a smaller transverse crack in the matrix which then extended along the inner radius at the center line resulting from hoop stress. At 816°C (Fig. 6 right), this material exhibited a number of radial cracks, some of which were branched, and others which were quite fine. Within one of the wider radial cracks, the 816°C sample also showed fracture occurring in

the interphase region, as shown by the matrix "trough" where a fiber had been pulled away (Fig. 7). The orientation of the specimen prevented EDS analysis.

At room temperature, the Sylramic-S300 sample exhibited several very narrow hoop cracks along the inner radius of the coupon, close to the center line. The cracks appear to have originated on opposite sides of the sample from the edge surface (Fig. 8). At one surface (Fig. 8, lower right) the source of the crack appeared to be a "notch" in the matrix. There was some evidence of crack branching, as well as fiber bridging. These cracks appear to lie mainly within the matrix material at the very surface. Note that the crack narrows significantly as it progresses (change of scale in figure). At 816°C, a

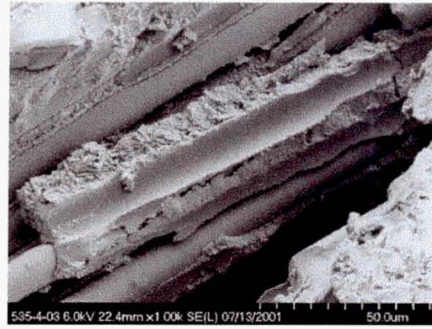


Figure 7. Interphase failure in a Sylramic/S300 coupon tested at room temperature. Area shown is within a wider radial crack.

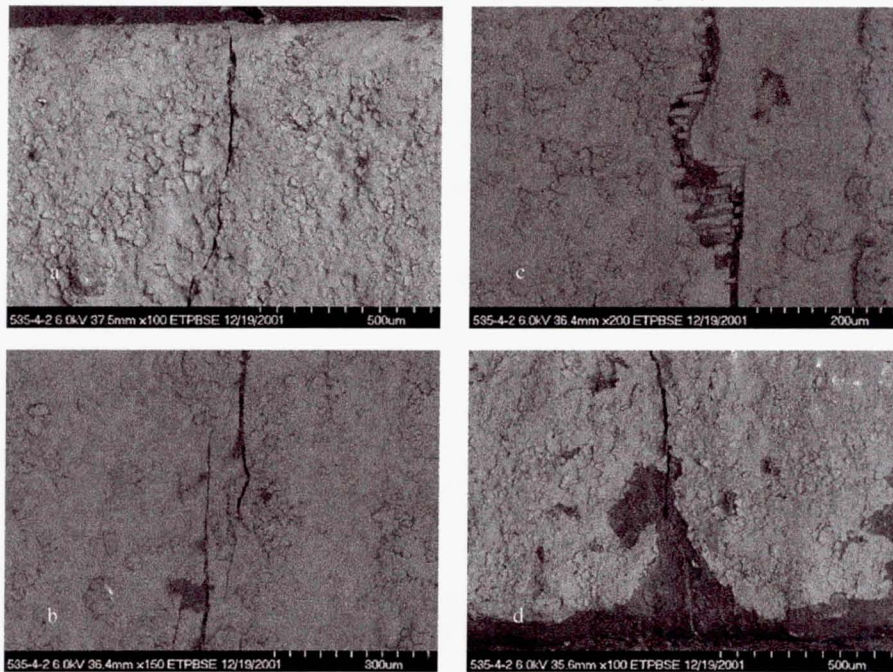


Figure 8. Hoop crack, starting on lower right, and stopping near a crack that originated on opposite edge (far left). Composite is Sylramic /S-300, tested at room temperature. Lettering indicates sequence; micrographs (a) and (d) are at opposite edges. A matrix chip, or "notch" can be seen in (d).

single, much narrower matrix hoop crack is observed. The ZMI/S200 coupons showed similar fracture behavior, but with fewer radial cracks and a single matrix hoop crack. A

Hi-Nicalon/S200 coupon tested at room temperature, which failed at very low stress, had few radial cracks and no discernable hoop crack.

SUMMARY AND CONCLUSIONS

The C-coupon geometry employed here produced interlaminar fracture, as characterized by a series of primarily parallel cracks through the thickness of the specimen and following the "C" curvature, consistent with the location of maximum radial stress predicted by finite element analysis. Fracture primarily occurred between the BN and CVI interphase layers for the Sylramic/ MI material, and the fiber and BN in the ZMI/MI composite. In the Sylramic/ S300 material, fracture also occurred at the interphase.

Almost all samples also showed much finer "hoop" cracks, parallel to the width of the specimen and very close to the 0° centerline, the position of maximum hoop stress as determined by finite element analysis. These are all very fine cracks, much narrower than the radial cracks, and are located in the unreinforced matrix material at the inner surface. As matrix cracking is known to occur at stresses very far below ultimate tensile stress in ceramic composites, these might have occurred very early in specimen loading, or may arise subsequent to interlaminar cracking as the hoop stress increases. Because the specimens were tested under "load control", but with a displacement limit to prevent them from being fractured in two pieces, they continued to be strained beyond the initial load drop; AE events were recorded beyond the "failure" load point. However, because these cracks are matrix, and do not appear to be producing fiber fracture, and as there is very close agreement between the room temperature ILT "button test" data and the calculated maximum radial stress, it is unlikely that they alter the primary finding of interlaminar tensile fracture.

The C-coupon geometry offers the opportunity to obtain ILT data at elevated temperatures. As the tensile strength of most CMCs is known to decrease with temperature, we cannot be certain that the requirement that ILT/tensile strength be less than 0.064 holds over the entire temperature range. However, fracture mode was not seen to change with temperature, except for the finding of fewer radial stress cracks at higher temperatures in the MI materials.

REFERENCES

1. Carlsson, L.A. and F. Ozdil, *Interlaminar Fracture of CMCs and Button Specimen Benchmark Testing, Task A6, High Speed Research/ Enabling Propulsion Materials Program, Final Technical Report*. October 31, 1999, NASA, Pratt and Whitney, GE Aircraft Engines.
2. Cui, G.Y. and C. Ruiz. *Through-Thickness Failure of Laminated C/Epoxy Composites under Combined Stress*. in *SEM Spring Conf. Exp. Mechanics*. 1994: Society for Experimental Mechanics, Bethel, CT.
3. Ko, W.L. and R.H. Jackson. *Multilayer Theory for Delamination Analysis of a Composite Curved Bar Subjected to End Forces and End Moments*. in *5th International Conference on Composite Structures*. 1989. Paisley, Scotland.
4. Lu, T.J., Z.C. Xia, and J.W. Hutchinson, *Delamination of Beams under Transverse Shear and Bending*. *Mater. Sci. Eng., A*, 1194. **188**(1-2): p. 103-12.
5. Abdul-Aziz, A., et al., *C-Coupon Studies of CMCs: Fracture Behavior and Microstructural Characterization*. *Ceram. Eng. and Sci. Proc.*, 2001. **22**(3): p. 569-576.

6. Hurwitz, F.I., et al., *C-Coupon Studies of CMC's: Fracture Behavior and Microstructural Characterization*. Ceram. Eng. Soc. Proc., 2001. **22**(3): p. 577-584.
7. Morscher, G.N., F.I. Hurwitz, and A.M. Calomino, *C-Coupon Studies of SiC/SiC Composites Part I: Acoustic Emission Monitoring*. Ceram. Eng. Sci. Proc., this volume, 2002.

C-COUPON STUDIES OF SIC/SIC COMPOSITES PART II: MICROSTRUCTURAL CHARACTERIZATION

Frances I. Hurwitz and Anthony M. Calomino

NASA Glenn Research Center

Gregory N. Morscher, Ohio Aerospace Institute

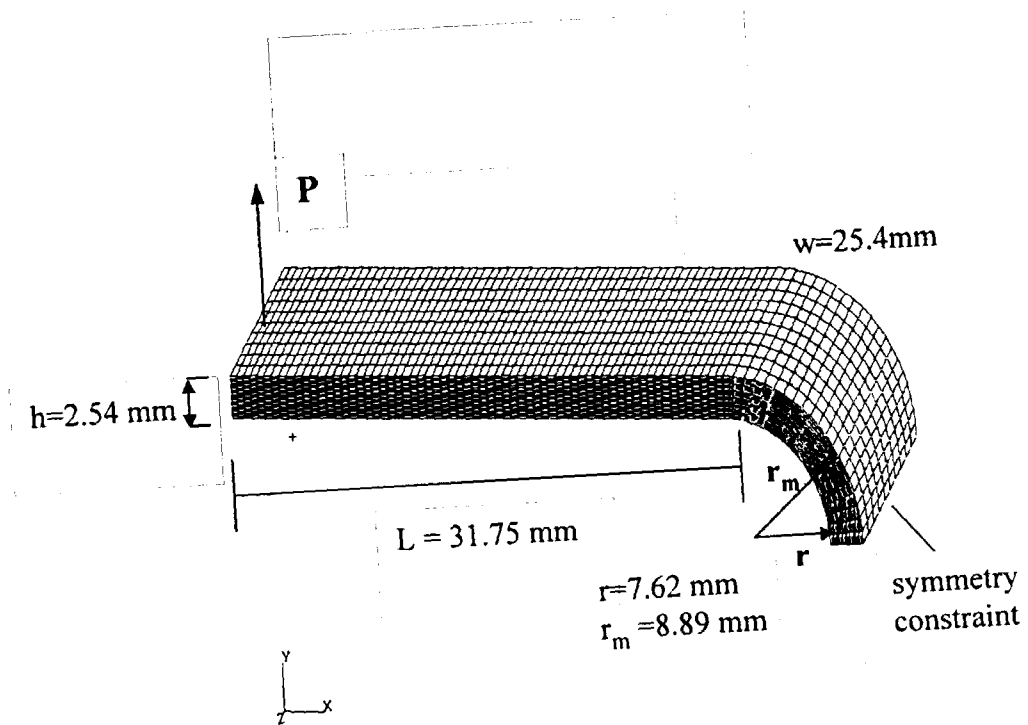
Terry R. McCue, QSS Group, Inc.



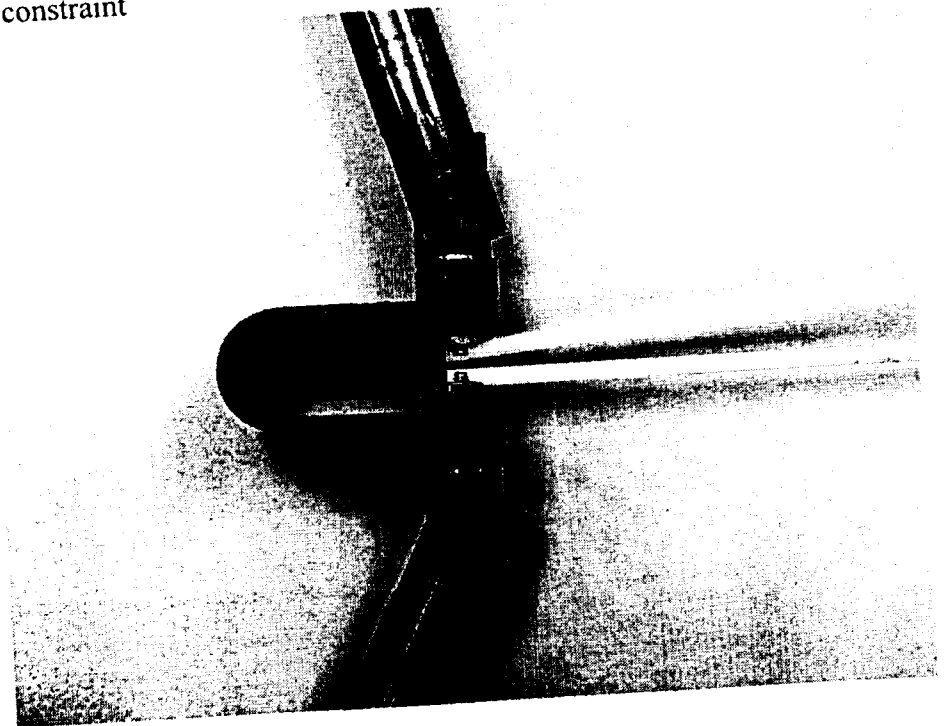
OBJECTIVE

- ◆ Development of an ILT test technique capable of use at elevated temperature.
- ◆ Evaluation of composite fabrication for components with bend radii.
- ◆ Characterization of fracture behavior in C-coupons at a variety of test temperatures for a number of different CMCs.





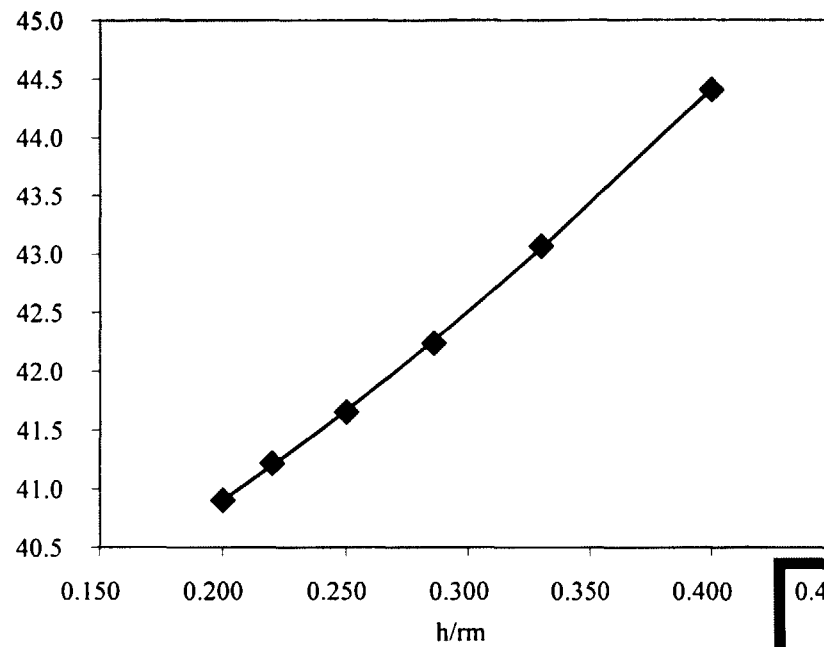
C-coupon geometry



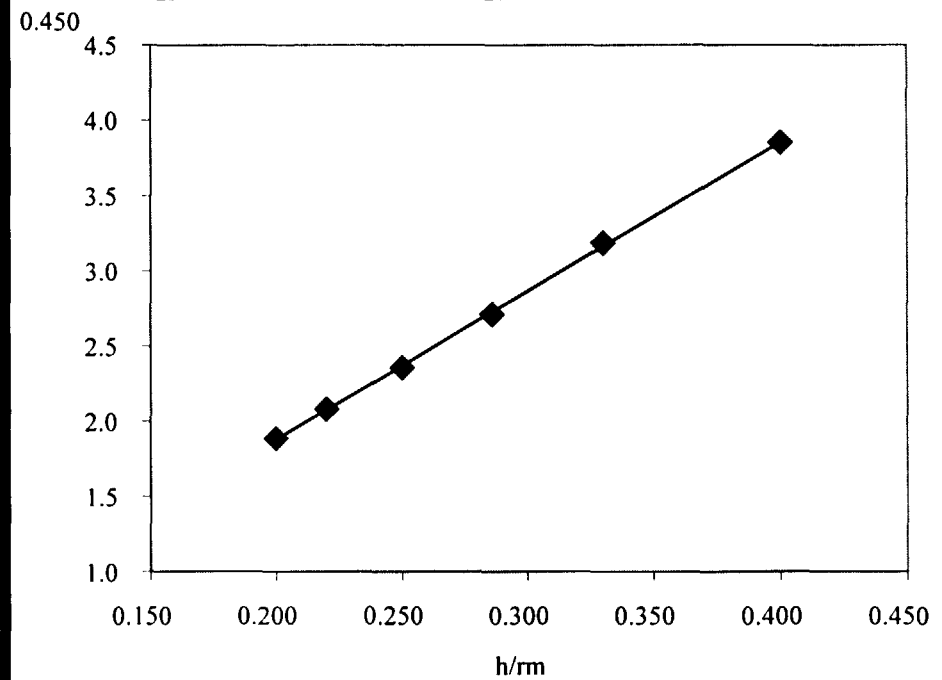
Necessary condition for delamination failure:

$$\frac{\text{radial stress}}{\text{hoop stress}} > \frac{\sigma_{\text{ILT}}}{\sigma_{\text{in-plane}}}$$

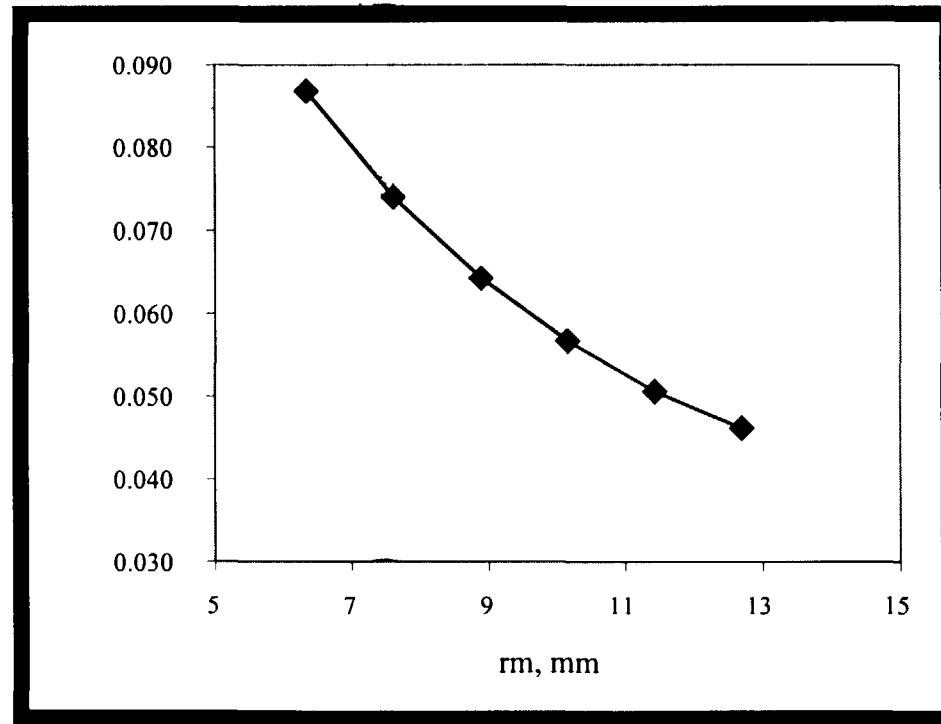
For geometry used here, radial stress/ hoop stress = 0.064.

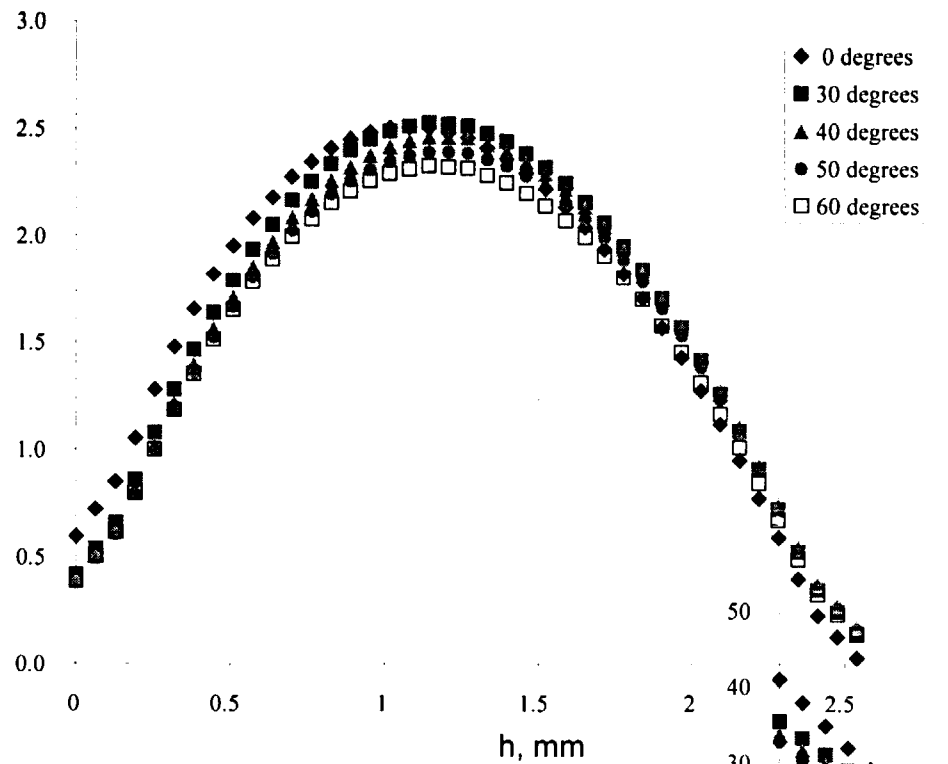


Stress vs. h/r_m

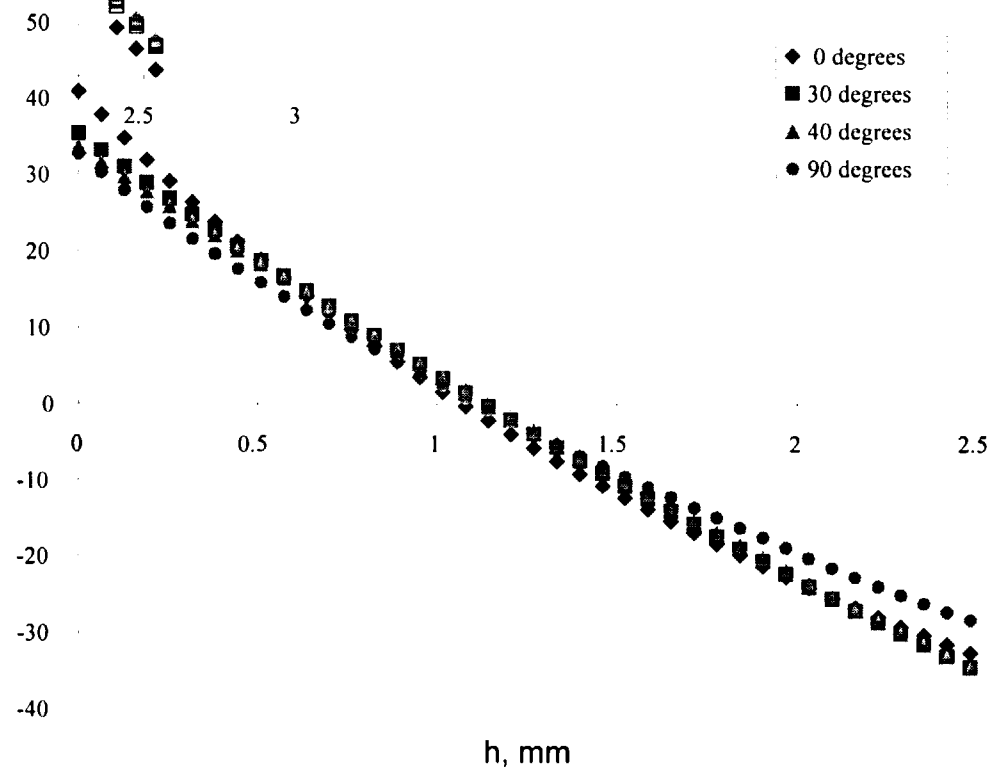


RATIO OF RADIAL TO HOOP STRESS AS A FUNCTION OF MEAN RADIUS





STRESS AS A FUNCTION OF COUPON THICKNESS



COMPOSITES

- ◆ Sylramic/ MI
- ◆ ZMI/ MI
- ◆ Sylramic/ S300
- ◆ ZMI/ S200
- ◆ Hi-Nicalon/ S200

TEST TEMPERATURES: 21, 816, 1204°C

Table I: Comparison of composite properties at room temperature.

Composite	Max Radial Stress, MPa	Max Hoop Stress, MPa	In- Plane Tensile Strength, MPa	ILT, MPa	ILT/Tensile
Sylramic/ MI	16.3 ± 1.0	269 ± 12	362 ± 25.5^1	15.5 ± 1.8	0.042
ZMI/ MI	12.5 ± 2.4^2	203 ± 39^2	N/A	N/A	N/A
Sylramic/ S300	15.9^3	265^3	317^4	11.9 ± 0.6	0.037
ZMI/ S200	12.7	170	162 ± 9.4^1	12.7 ± 2.7	0.078
HiNicalon/ S200	8.5	120	248^4	6.9^4	0.027

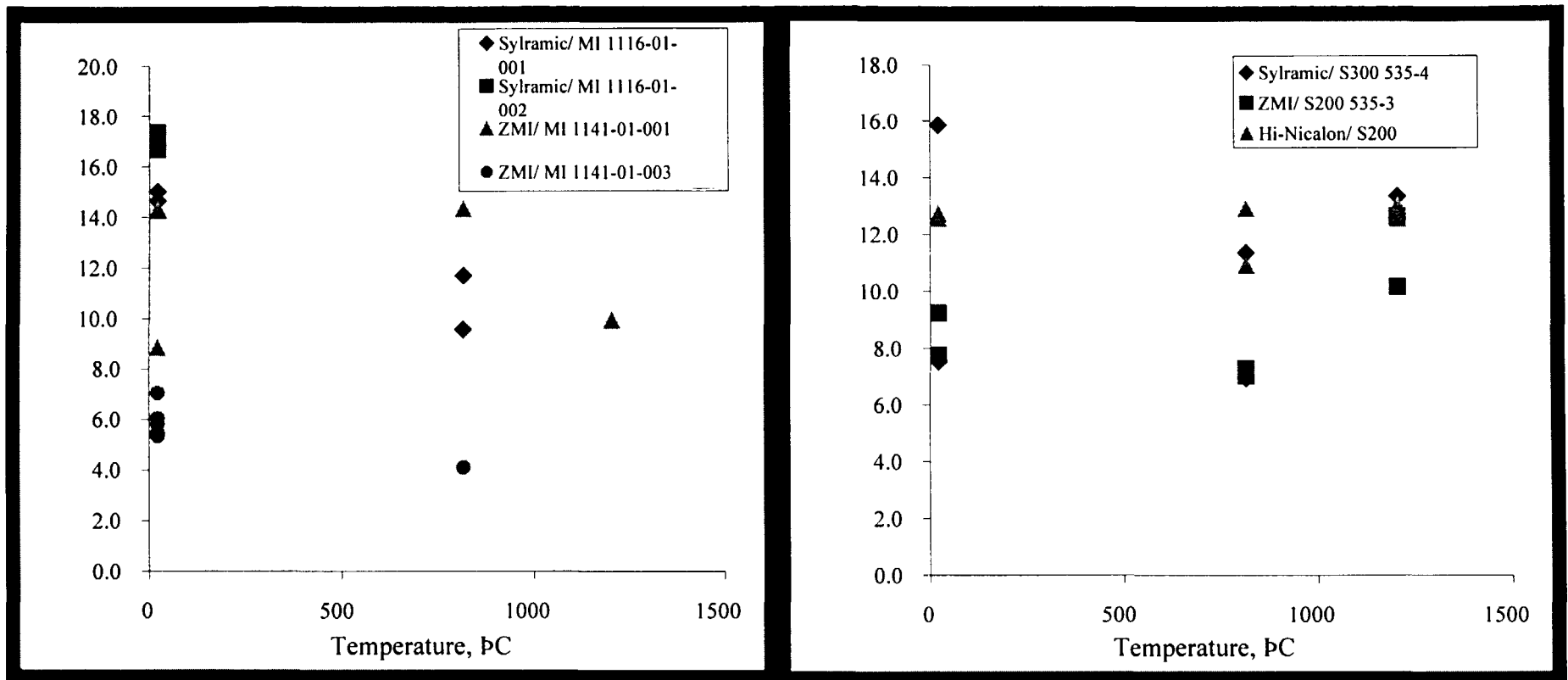
¹ 816IC data.; room temperature strength expected to be equal or higher.

² Data is from one log only; the second log contained large pores.

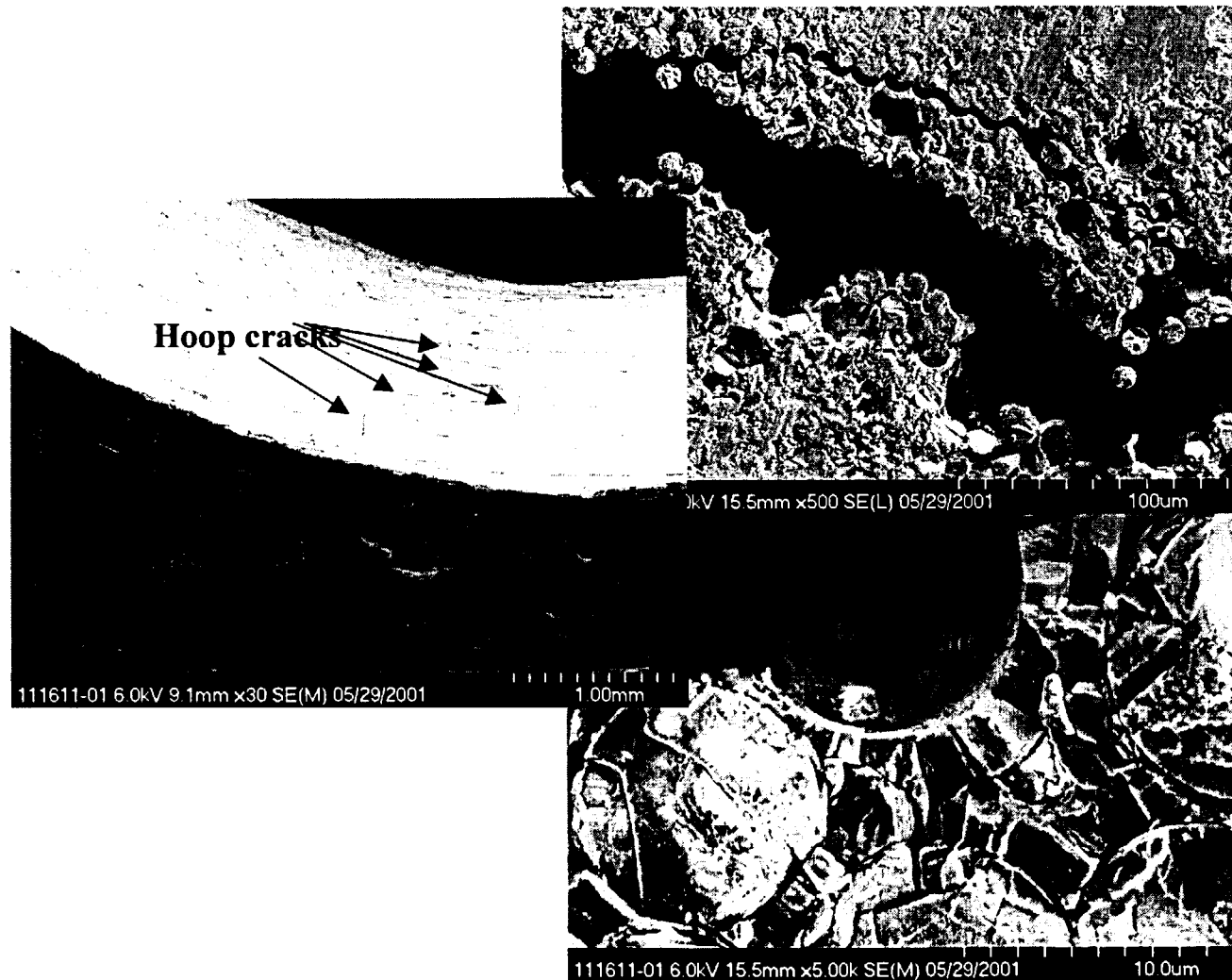
³ Single data point—second sample failed at very low stress.

⁴ COI data.





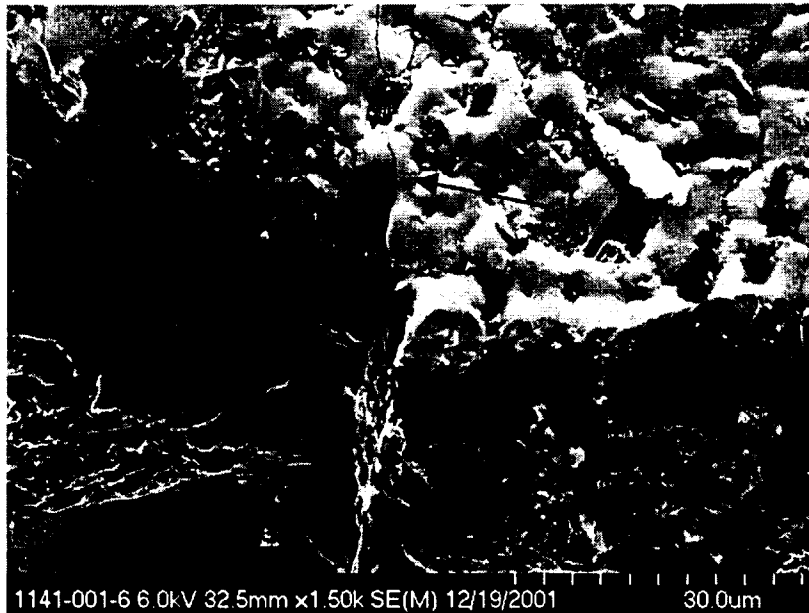
MAXIMUM RADIAL STRESS VS. TEMPERATURE



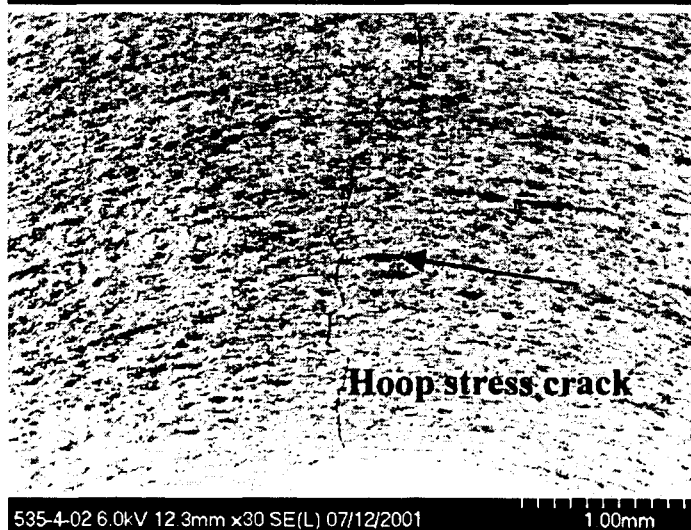
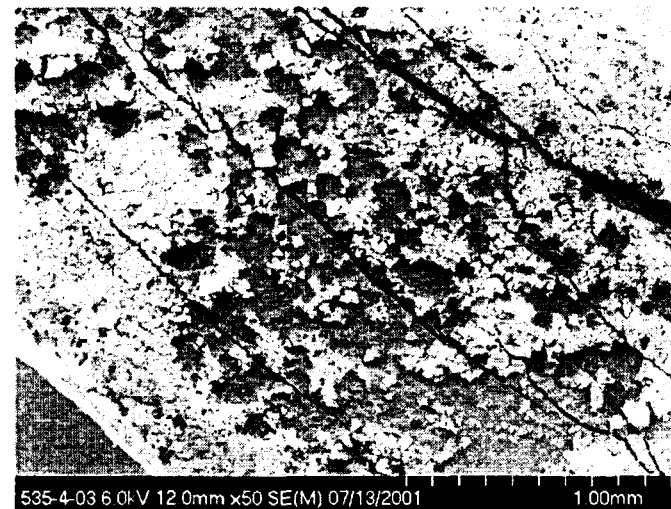
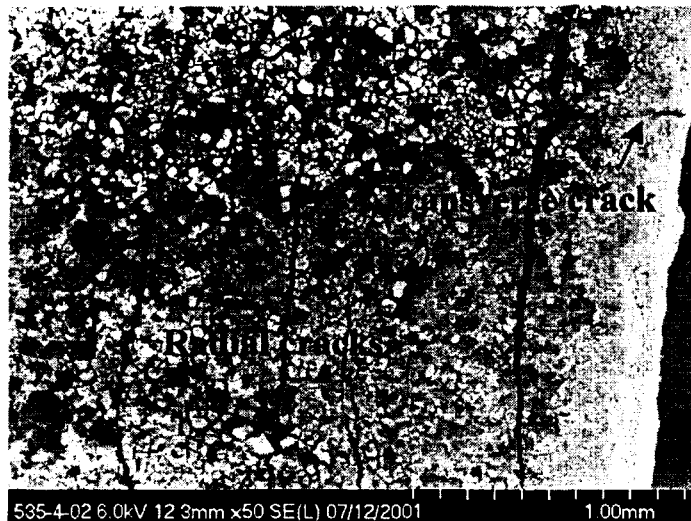
ROOM TEMPERATURE FRACTURE, SYLRAMIC/ MI



**SYLRAMIC MI, TESTED AT 816°C.
NOTE DECREASED NUMBER OF RADIAL STRESS
CRACKS COMPARED TO RT**



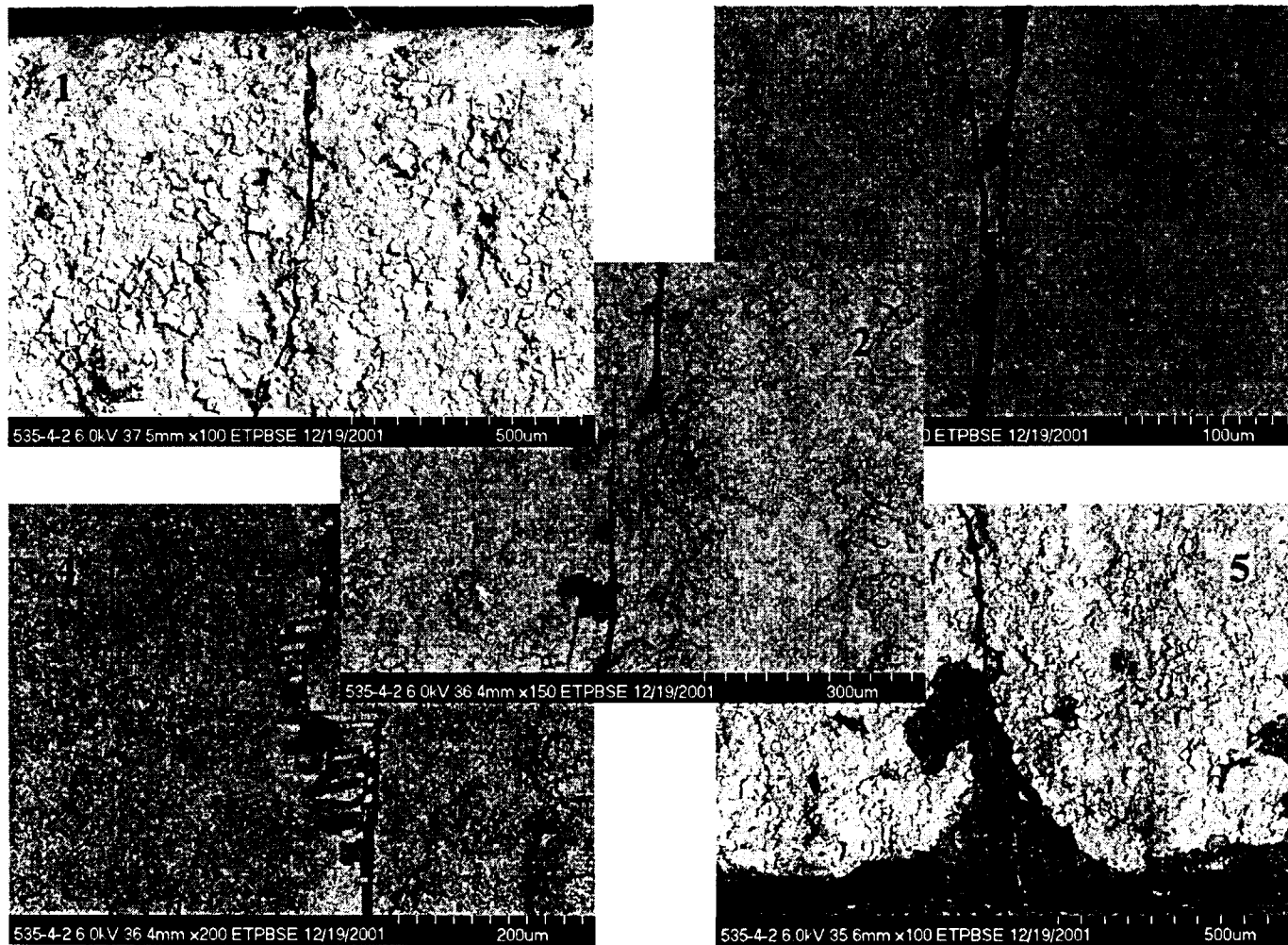
**ZMI/ MI ROOM TEMPERATURE, HOOP STRESS CRACK
ON INNER RADIUS**



Room Temperature

816°C

SYLRAMIC/ S300



**SYLRAMIC/ S300 ROOM TEMPERATURE HOOP STRESS
CRACK, INNER RADIUS**

SUMMARY AND CONCLUSIONS

- ◆ C-coupon geometry used here was able to be tested at 21, 816 and 1204°C.
- ◆ Interlaminar fracture (cracks due to radial stress) were the dominant failure mode in all tests.
- ◆ Radial stress induced cracks produced failure at the interphase (between BN and fiber, or BN and matrix).
- ◆ In the MI materials, the number of radial cracks appeared to decrease with temperature.
- ◆ Fine cracks on the inner radius, close to the centerline, were observed in almost all coupons (exception: Hi-Nicalon S200). These were surface cracks in the matrix, arising from hoop stresses.



SUMMARY AND CONCLUSIONS (CONT'D)

- ◆ All samples contained multiple radial stress cracks. Although maximum radial stress is at mid-thickness, the sequence of cracking could not be determined precisely.
- ◆ There is good agreement between the maximum radial stress at failure in the C-coupon and the ILT strength as determined from the “button test” (ASTM 1468).

